Eliminating the Residual Ultraviolet Excitation Light and Increasing Quantum Dot Emission Intensity in LED Display Devices

Caiman Yan, Guanwei Liang, Guoquan Liu, Yong Tang, Jiasheng Li, and Zong-Tao Li, *Member, IEEE*

***Abstract*— Ultraviolet light-emitting diodes (UVLEDs) used as excitation sources for quantum dots (QDs) are promising candidates for the display field. To eliminate the residual excitation light, the conventional method is simply increasing the optical density of QDs for packaging, which would significantly reduce the luminous efficiency of QD-light-emitting diode (LED) devices owing to reabsorption loss. In this study, the combination strategy of a boron nitride (BN) reflective coating and an ultraviolet-reflection filter (UV-R filter) for QD-LED devices is proposed. By managing the recycle of UV light to excite more QDs and reducing the reabsorption effect of QDs carefully, their green emission intensity of LED using such a strategy is 82.0% higher than that of a conventional device with a similar QD light energy proportion of ∼99.0% (almost no residual UV excitation light). This strategy is also effective for red QD-LED devices while eliminating residual UV excitation light and enhancing the red emission intensity. Therefore, this study provides an effective way to develop QD-LED devices with high QD emission intensity and low UV light leakage for display.**

***Index Terms*— Light-emitting diodes (LEDs), optical performance, quantum dot (QD), residual ultraviolet (UV) excitation light, UV.**

I. Introduction

LIGHT-EMITTING diodes (LEDs) are showing an explosive growth trend in the display and lighting fields as a result of their high brightness, good stability, long life, and contribution to environmental protection [1], [2]. Red, green, and blue (RGB) are the three primary additive colors in display technology. To obtain text or images in color, conventional backlighting typically uses white LEDs as the light source and optical filter technology to obtain the colors [3]. A limitation of using white LEDs for backlighting is that it is difficult to obtain a black image with a satisfactory contrast ratio. By employing a large number of LED chips, RGB direct display technology is able to use local dimming techniques [4], which can attain a better contrast ratio and become one of the most promising techniques in the high-quality display.

RGB LED devices are the basis of direct display technology [5]. Because the blue LED is an advanced technology, it is usually employed for blue light [6]; for the green and red light, an effective strategy is to use shorter wavelengths to excite fluorescent material [7]. Quantum dots (QDs) are an attractive alternative to fluorescent material because of their select emission wavelength, narrow full-width at half-maximum (FWHM), and high color purity [8], [9]; there has been a surge of attention on applying QDs in the display field. Luo *et al.* [10] reported that the color gamut could reach 115% NTSC(1931) using QDs. Similar wide color gamut results have been confirmed by Zhu *et al.* [11] and Chen *et al.* [12]. However, the luminous efficiency of QD-LED devices is not as high as that of traditional phosphor materials such as yttrium aluminum garnet (YAG) [13]. Many studies have focused on improving QD luminous efficiency [14]. Lei *et al.* [15] reported an optimized single-unit structure to enhance the optical performance of QD-LED devices; our team found that using the hexagonal pore structure of SBA-15 mesoporous particles for package enhances the color-conversion efficiency of QD-LED devices by more than 50% [16]. Although the luminous efficiency of QD-LED devices has increased, it is still difficult to satisfy the requirement in RGB display.

For an excitation light source, short wavelengths are mainly obtained from LED chips, including ultraviolet (UV) and blue chips. In our previous research, we have compared the display performance of LED devices using UV and blue chips as short-wavelength excitation light sources [17]. The UV-excited QD LED devices exhibit a better color purity compared with the blue-light excitation counterparts. For example, at the same QD concentration of 1.2 wt%, the residual UV light of the UV-excited LED is 30.5%, while the residual blue light of the blue-excited LED is 46.7%. Moreover, by using UV light as the excitation source, the color gamut of the UV-excited LED could be increased to 110% NTSC1953

Manuscript received August 20, 2020; revised October 11, 2020; accepted December 9, 2020. Date of publication January 1, 2021; date of current version January 22, 2021. This work was supported in part by the Science and Technology Program of Guangdong Province under Grant 2019B010130001, in part by the National Natural Science Foundation of China under Grant 51775199 and Grant 51735004, and in part by the Fundamental Research Funds for the Central Universities. The review of this article was arranged by Editor X. Guo. *(Corresponding authors: Jiasheng Li; Zong-Tao Li.)*

Caiman Yan, Guanwei Liang, Guoquan Liu, and Yong Tang are with the National and Local Joint Engineering Research Center of Semiconductor Display and VLC Devices, South China University of Technology, Guangzhou 510641, China.

Jiasheng Li and Zong-Tao Li are with the National and Local Joint Engineering Research Center of Semiconductor Display and VLC Devices, South China University of Technology, Guangzhou 510641, China, and also with Foshan Nationstar Optoelectronics Company Ltd., Foshan 528000, China (e-mail: jiasli@foxmail.com; meztli@scut.edu.cn).

Color versions of one or more figures in this article are available at https://doi.org/10.1109/TED.2020.3044556.

Digital Object Identifier 10.1109/TED.2020.3044556

0018-9383 © 2021 IEEE. Personal use is permitted, but republication/redistribution requires IEEE permission.
See https://www.ieee.org/publications/rights/index.html for more information.

Authorized licensed use limited to: SOUTH CHINA UNIVERSITY OF TECHNOLOGY. Downloaded on April 06,2021 at 08:55:24 UTC from IEEE Xplore. Restrictions apply.

standard, while the color gamut of the blue-excited LED is only about 85% NTSC1953 standard. These results suggest that the UV excitation solution has an advantage in the display field with better color purity and a wider color gamut [17]. However, one of the great challenges in short-wavelength excitation is eliminating its residual peak [18]. In pursuit of green or red light, the residual short-wavelength excitation light hinders color purity improvement. What is worse, the mammalian cell is more sensitive to short wavelengths such as blue or UV light [19], [20]; the American Medical Association has issued a warning against long-term exposure to these short-wavelength light [21]. To eliminate the residual short-wavelength excitation light, Chen *et al.* [22] designed a monolithic RGB micro-LED chip, with a hybrid Bragg reflector (HBR) and a distributed Bragg reflector (DBR) on the bottom and topside, achieving the elimination of blue light when green light and red light are excited. This solution considers only the chip design and has not conducted research from the device package integration level. In the device package, Lin *et al.* [23] also introduced a specially designed DBR structure, which allows the visible (VS) light to pass but hinders the residual UV excitation light. However, the cost would increase with complicated DBR manufacturing. Meanwhile, the UV light blocked by the DBR can be easily absorbed by QDs; the reexcitation of QDs can also increase the conversion loss owing to the more serious reabsorption effect [24]. At present, most of the previous research studies considered only the short-wavelength light eliminating or the conversion efficiency separately, and there are still great challenges to simultaneously eliminate residual UV excitation light while increasing QD emission intensity.

In this study, two different LED structures to eliminate the residual UV excitation light are compared. The first conventional structure eliminates the residual UV excitation light only by increasing the optical density (LED I). A combined structure of a boron nitride (BN) reflective coating and a UV-reflection filter (UV-R filter) for LED is proposed as our structure (LED II). The effect of the QD concentration on the elimination of residual UV excitation light and the color conversion is studied first. Then the proposed LED II with the combination of a UV-R filter and BN coating is optimized to enable the secondary excitation of QDs while eliminating the residual UV excitation light. Moreover, the severe reabsorption problem from QDs caused by UV light recycling is solved by regulating the QD concentration. Finally, the proposed LED II device has a QD emission intensity 82.0% higher than traditional LED I under a similar QD light energy proportion (QP) of ~99.0% according to a comprehensive comparison.

II. Experimental

A. Materials and Equipment

The green and red QDs (GQDs and RQDs) were purchased from Beijing Beida Jubang Science and Technology Company, Ltd., with a labeled photoluminescence quantum yield (PLQY) of over 90%. Polydimethylsiloxane (PDMS) was purchased from Dow Corning Corporation, USA. The optical filters

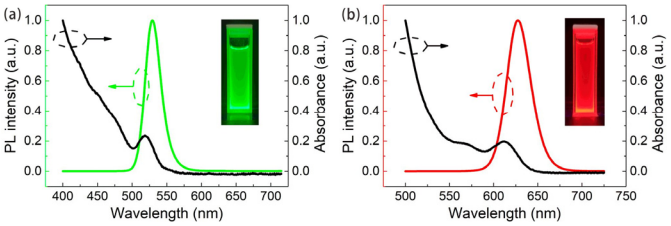

Fig. 1. PL and absorption spectra of (a) GQDs and (b) RQDs.

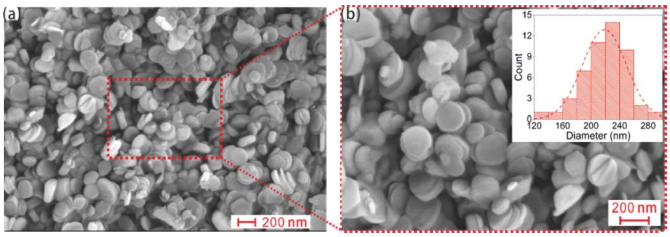

Fig. 2. SEM image of BN NPs: magnification (a) 30 K and (b) 50 K. Inset is a calculation of the diameter distribution of 50 samples.

(bandpass and dichroic filter) were designed by PHTODE Company, Ltd. The high purity BN nanoparticles (BN NPs) were purchased from Shanghai Xiangtian Nano Materials Company, Ltd. In detail, the GQDs and RQDs are nanoscale fluorescent materials based on a CdSe/ZnS core–shell structure. Their photoluminescence (PL) and absorbance spectra are shown in Fig. 1. The emission wavelengths of the GQDs and RQDs are 529 and 627 nm, respectively. Their FWHM values are 27 and 31 nm, respectively, which are much narrower than that of the common YAG phosphor [25]. QDs with narrow FWHM have great potential for displays because of their high color purity, as shown in the inset in Fig. 1. In addition, the absorption peaks of the GQDs and RQDs are located at 519 and 612 nm, respectively.

As for BN NPs, they appear stacked in layers as shown in Fig. 2(a). Under greater magnification [Fig. 2(b)], the BN NPs are approximately circular and sheet-like. Based on a sample of 50 NPs, the size distribution of the BN NPs is approximately normal, with an average diameter of 218.7 nm.

To eliminate the residual UV excitation light, the dichroic filter is chosen here. A dichroic filter is of the cutoff type, meaning that wavelengths shorter than its threshold are not passed. The transmittance shown in Fig. 3(a) confirms this characteristic. In particular, the dichroic filter transmits for wavelengths of over 512 nm with a transmittance of up to 90%. The transmittance in other wavelength regions is close to zero like the UV band (370 nm). Moreover, the reflectance of the dichroic filter was also measured [Fig. 3(a)]. The regularity of the reflectivity is exactly the opposite of the transmittance. Using $BaSO_4$ as the 100% reflection baseline, the reflectivity of the dichroic filter is up to 100% in the band within 350–450 nm. Therefore, this dichroic filter mainly filters UV light by reflecting. Based on this experimental conclusion, the dichroic filter is referred to as the UV-R filter. The UV-R filter plays a key role in blocking UV while transmitting VS light from QDs, as shown in Fig. 3(b).

The PL and absorbance spectra were measured using a fluorescence spectrophotometer (RF-6000, Shimadzu, Japan) and a UV-VS spectrophotometer (TU-1901, Persee, Beijing,

Authorized licensed use limited to: SOUTH CHINA UNIVERSITY OF TECHNOLOGY. Downloaded on April 06,2021 at 08:55:24 UTC from IEEE Xplore. Restrictions apply.

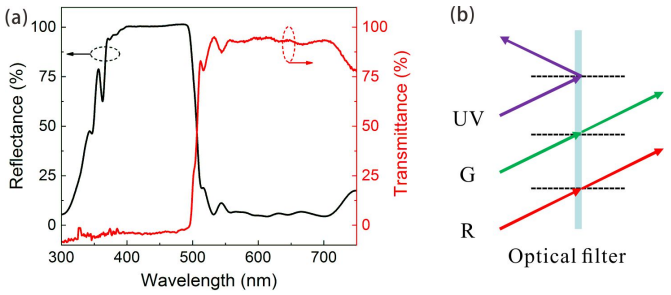

Fig. 3. (a) Transmittance and reflectance spectra of the dichroic filter. (b) Schematic of UV-R filter function.

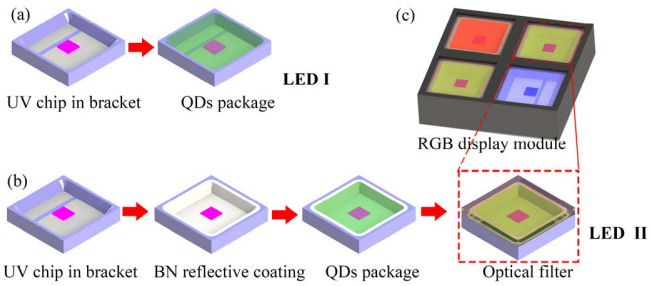

Fig. 4. (a) and (b) Schematics of two LED structures. (c) Schematic of the RGB display module applying LED II structure in red and green LED devices.

China). The image of the BN NPs was captured by a scanning electron microscope (SEM) operating at 10 kV (Merlin, Zeiss, Oberkochen, Germany). Electroluminescence (EL) spectra and optical parameters were obtained by a calibrated spectral test system, primarily composed of a high precision power supply (Keithley 2425, Keithley Instruments and Products, Cleveland, OH, USA), an integrating sphere, an Oceanic spectrometer (USB2000+, Ocean Optics, Largo, FL, USA), and corresponding software. The transmission and reflection spectra were obtained by a UV–VS spectrometer with integral sphere attachments (UV-Vis 2600, Shimadzu, Japan). For the reflection spectra of an optical filter, an incidence angle of 8° was adopted for the experiment. Thermal tests were performed using an infrared thermal imaging instrument (A655SC, FLIR SYSTEMSAB, Switzerland).

B. Preparation of QD-LED Devices With a UVLED Chip

To prepare the green or red QD-LED devices, a 45 mil × 45 mil UV LEDs (UVLEDs) chip with a 370-nm emission peak was first mounted on the substrate. Gold wired electrical connections were made by ultrasonic welding. PDMS silicone was chosen as the major packaging material. Herein, two types of LEDs were prepared by using BN-based and QD-based silicone. The BN-based silicone was formed by mixing BN NPs and PDMS together in specific mass ratios. For the BN reflective coating, a high-precision dispensing machine is used to uniformly dispense the BN-based silicone around the stent. This dispensing quality of BN-based silicone is controlled at 3 mg ± 0.1 mg. Then this BN-based silicone was flowed along the edges to the bottom of the bracket. Taking advantage of the colloidal fluidity, the entire bottom and sides of the bracket (excluding the LED chip) were covered with the BN reflective coating. As for the QD coating, the preparation of the QD-based silicone is similar to that of BN-based silicone, which was directly dispensed into the cavity; the optical filter was then placed on top of the LED device and joined by a PDMS connection. Finally, the LED device was heated at 90 °C for 1 h. To maintain experimental consistency, the amount of silicone was fixed at 11 mg, which was formed by 11-mg QD-based silicone alone or a combination of 8-mg QD-based silicone and 3-mg BN-based silicone.

As shown in Fig. 4(a) and (b), there are two kinds of LEDs to be explored in this study. LED I denotes an LED device that contains only QDs package, which is also the most common traditional packaging structure; LED II is fabricated by first introducing the BN reflective coating, then filling the QD-based silicone and finally combining with an optical filter. As shown in Fig. 4(c), a typical RGB display module includes three primary color LED devices. Blue light is from a blue LED chip; green and red light are obtained by exciting QDs with UV light. By applying the LED II structure to UV-excited green and red LEDs, it is expected to obtain a pure three primary colors without residual UV excitation light and high QD emission intensity. By adjusting the ratio of the three primary colors, full display colors could be obtained. In this research, we mainly focused on the optical performances of the single unit in an RGB display module.

III. Results and Discussion

A. Effect of QD Concentration on Device Color Purity and QD Emission Intensity

For a high-quality display device, it is essential to reduce the residual UV excitation light and enhance the QD emission intensity as much as possible, which is also the primary goal of the above LED structures (Fig. 4) in this study. The first LED structure represents the idea of increasing the optical density (high QD concentration) for UV excitation light. However, this strategy is barely investigated comprehensively considering the elimination of excitation light and the enhancement of QD emission intensity. Therefore, we first investigated traditional LED I structure to provide a better guideline on the subsequent design of our proposed LED II [Fig. 4(b)].

Herein, we use the LED I structure with GQDs as an example to investigate the effect of QD concentration of eliminating residual UV excitation light and enhancing QD emission intensity. A series of green LEDs with different QD mass concentrations 0, 0.08, 0.16, 0.4, 0.6, 1.6, 3.2, and 4.8 wt% was fabricated. From the EL spectra in Fig. 5(a), each QD-LED device has a UV peak (371 nm) and a green peak. The UV peak is derived from the UV LED chip, and the green peak originates from GQDs. As the concentration of QDs increases, the intensity of UV light decreases, while the intensity of QD light initially rises and then falls, reaching the maximum at 0.6 wt% concentration. In addition, the wavelength of the QD light at high concentration is accompanied by a redshift. When the UV and green peaks are analyzed separately in Fig. 5(b), the UV intensity is close to 0 at a high QD concentration of 4.8 wt%, and the green intensity obtains a maximum radiant flux at 0.6 wt%. At a low QD

Authorized licensed use limited to: SOUTH CHINA UNIVERSITY OF TECHNOLOGY. Downloaded on April 06,2021 at 08:55:24 UTC from IEEE Xplore. Restrictions apply.

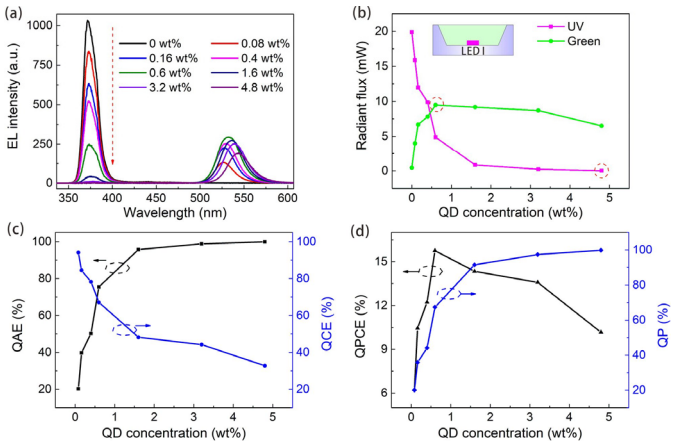

Fig. 5. (a) EL spectra. (b) UV/green light intensity. (c) QAE and QCE. (d) QPCE and QP of QD-LED devices with different QD concentrations.

concentration, much more UV light converted into QD light follows the increase of QD concentration. However, when the concentration becomes too high, reabsorption effect of QDs dominates, accompanied by the reabsorption and reemission of photons. This process results in energy loss and reduces the QD emission intensity [26].

The process of color conversion is mainly divided into two steps: absorbing UV light and then converting it into QD emission light. To better discuss these processes and evaluate the performance of QD-LED devices, QD absorption efficiency (QAE), QD conversion efficiency (QCE), QP, and QD power conversion efficiency (QPCE) are defined as follows:

$$\mathrm{QAE} = \frac{I_{\mathrm{ab}}}{I_{\mathrm{UV}}} \tag{1}$$

$$\mathrm{QCE} = \frac{I_{\mathrm{QD}}}{I_{\mathrm{ab}}} \tag{2}$$

$$\mathrm{QP} = \frac{I_{\mathrm{QD}}}{I_{\mathrm{Total}}} \tag{3}$$

$$\mathrm{QPCE} = \frac{P_{\mathrm{QD}}}{P_E} \tag{4}$$

where I_{ab} indicates the absorbed UV intensity by QDs; I_{UV} means the initial UV intensity of a UVLED chip; I_{QD} means the QD emission intensity; I_{Total} means the total emission intensity of a LED; P_{QD} represents the QD optical power; and P_E means the electric power of a LED. The calculated intensity is obtained by integrating the EL spectrum obtained from the experiment. Specifically, the QAE represents the QD absorption capacity; the QCE represents the QD color conversion efficiency; the QPCE represents the total energy efficiency of QDs converting electrical power to optical power; the QP represents the amount of residual UV excitation light. A higher QP means less residual UV excitation light, indicating better color purity.

The QAE, QCE, and QPCE, QP of LEDs with different QD concentrations are concluded and shown in Fig. 5(c) and (d), respectively. As shown in Fig. 5(c), the QAE increases while QCE decreases with increasing QD concentration, which indicates that QAE and QCE have a negative relationship. At a lower QD concentration, LED owns a higher color conversion efficiency while weaker absorption ability to the UV light. For example, at the lowest QD concentration, QCE is 94.1% and QAE is only 20.2%. Therefore, there is a tradeoff between QAE and QCE for QD emission intensity. As shown in Fig. 5(d), QPCE first increases to the highest value of 13.4% at a QD concentration of 0.6 wt% and then decreases, which is consistent with the QD emission intensity [Fig. 5(b)]. Meanwhile, the QP of LEDs keeps increasing with increasing QD concentration. As a result, the LED device attains a QP of 99.2% at a QD concentration of 4.8 wt%. As the elimination of residual excitation light is necessary for high-quality display applications, the QD concentration of 4.8 wt% is optimal for LED I. However, eliminating the residual UV excitation light at such a high QD concentration would inevitably sacrifice the QCE. The QCE decreases by 34.4% when QD concentration further increases from 0.6 wt% (where is the maximum QPCE) to 4.8 wt% (where is the maximum QP). Therefore, it is still of great challenge to simultaneously obtain high QP and QPCE at the same time, which is also the pursuit of this study.

B. Proposed a Combined Structure for Eliminating Residual UV Excitation Light While Increasing QD Emission Intensity

An optical filter is widely used in backlighting, which is recently introduced to eliminate the residual short-wavelength excitation light in LED devices [27]. In a previous study, it was found that the BN NPs do not absorb 370-nm UV light due to their excellent wide bandgap properties [28]. Therefore, a combined structure of a BN reflective coating and a UV-R filter has been introduced here to further investigate the performance of reducing residual UV light, which is the LED II described in the experimental stage [Fig. 4(b)]. According to Section III-A, an optimal QD concentration of 0.6 wt% is used for LED II packaging.

The EL spectra of LED II with different BN concentration coatings were tested and shown in Fig. 6(a). In our cases, the maximum BN concentration for BN coating is set to 15 wt%, which is limited to the high viscosity. The UV-R filter maintains excellent reflection performance for the UV light so that the UV light of all samples is close to zero. Meanwhile, the QD emission intensity of LEDs increases as BN concentration increases; with 15 wt% BN concentration coating, the QD emission intensity further increases by 20.1% compared with that of LED II (UV-R filter). The behind mechanisms would be discussed in subsequence. Moreover, the QPCE and QP are also calculated here, as shown in Fig. 6(b). The QP of LED II is maintained at a very high value of over 98%. Moreover, the QPCE further increases from 15.3% to 18.3% as the BN concentration increases from 0 to 15 wt%. For QD-LED, the QPCE is mainly related to UV intensity and QD emission intensity. Since the UV peak of all samples is close to 0, the increase of QPCE is mainly due to the increase of QD intensity, which is attributed to the introduction of BN coating. These results suggest that the BN coating is essential to eliminating residual UV excitation light while further improving the QD emission intensity.

To investigate the effect of BN coating for the LED II, UVLEDs (without packaging QDs) with different BN concentration coatings were fabricated and discussed. Their EL

Authorized licensed use limited to: SOUTH CHINA UNIVERSITY OF TECHNOLOGY. Downloaded on April 06,2021 at 08:55:24 UTC from IEEE Xplore. Restrictions apply.

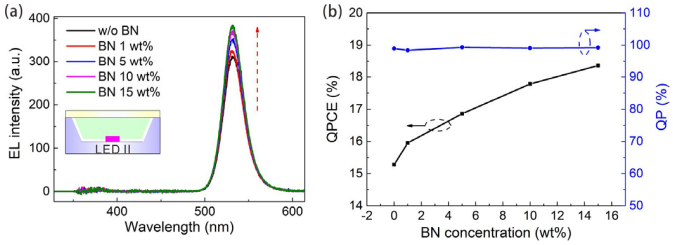

Fig. 6. (a) EL spectra. (b) QPCE and QP of LED II with different BN concentration coatings.

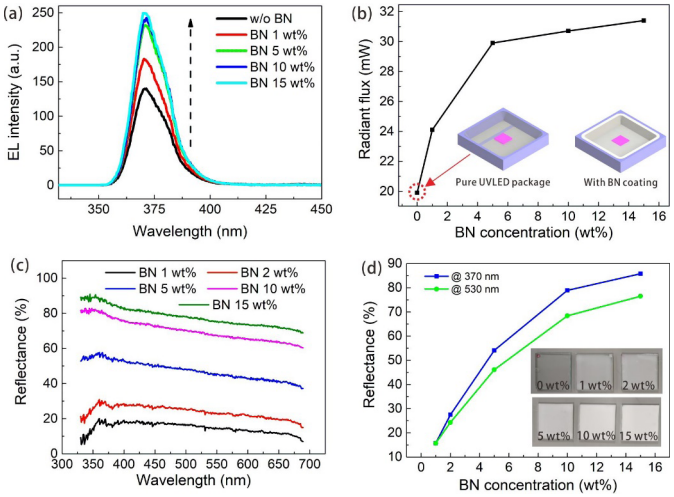

Fig. 7. (a) EL spectra. (b) Radiant flux of UVLEDs with different BN concentration coating, inset shows the schematic of UV LED with or without BN coating. (c) Reflectance spectra. (d) Specific reflectance at 370 and 530 nm of BN films with different BN concentrations, inset shows the physical graph of the corresponding BN film.

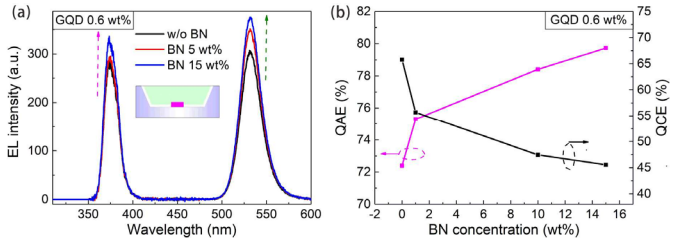

Fig. 8. (a) EL spectra. (b) QAE, QCE of LEDs removing UV-R filter. The QD concentration is set as 0.6 wt% here.

spectra are shown in Fig. 7(a). The UV intensity keeps rising as BN concentration increases. The radiant flux is concluded in Fig. 7(b). Specifically, the best radiant flux improvement is 57.8% with 15 wt% BN concentration coating, compared with the UVLED without BN coating. Therefore, the BN coating reduces the internal loss of UV light and improves the overall light output of the UVLED device. A previous study pointed out that the conventional TiO_2– based polymer brackets used for blue LEDs are no longer suitable for UVLEDs, which has a relatively severe light absorption effect [29]. Therefore, it is speculated that the BN NPs with a wide bandgap form a special layer of high reflectivity, which reduces the absorption loss of the polymer bracket. A series of BN films with a concentration ranging from 0 to 15 wt% were prepared on a glass substrate to support this notion; the BN film thickness is set to 150 μm. The reflection spectra of the BN films are given in Fig. 7(c). With the addition of BN NPs, the reflectances of all wavelengths gradually increase, and the increase rate of the UV region is more obvious than the VS region. As shown in the inset in Fig. 7(d), without BN NPs, the film is highly transparent. Specifically, the UV reflectance of BN film could increase to 85.8% with 15 wt% BN concentration at 370 nm. Therefore, BN coating in UV LED devices mainly plays a role in blocking the bracket from absorbing UV light and enhancing the reflection of UV light. In short, this high reflective BN coating strategy could increase the total amount of initial UV light intensity, probably leading to much more QD excited and thereby increasing the QD emission intensity. Meanwhile, as shown in Fig. 7(d), it is found that the reflectance at the green light wavelength (530 nm) is also gradually increasing; the reflectance of green light increases to a high value of 76.5% for a BN concentration of 15 wt%. These results demonstrate that the BN coating with high concentration also has an excellent reflectivity on QD light, which is helpful to reduce the backward emission loss of QD light.

Furthermore, the QD is added into consideration to investigate the effect of BN coating on color conversion. Herein, the UV-R filter is removed to test the EL spectra of the LEDs, as shown in Fig. 8(a). With the increase of BN concentration, both the UV intensity and the QD emission intensity increase. At a BN concentration of 15 wt%, the UV and QD emission intensity increase by 15.9% and 20.3%, respectively, compared to the LED sample without BN coating. As discussed in Fig. 7, the BN coating could increase the reflection of UV light, thereby increasing the QD excitation, which is also supported by the QAE concluded in Fig. 8(b). The QAE of all BN-coated LED samples is higher than that of the reference samples without BN coating. In particular, the QAE of the LED with 15 wt% BN concentration is 79.7%, which is 7.3% higher than of the LED without BN coating. Therefore, the BN coating is also beneficial to increase the QAE, which means that much more UV light could be absorbed by QDs. Actually, the QD emission intensity (I_{QD}) is a major concern in this study. According to (1) and (2), I_{QD} can be calculated by the following formula:

$$I_{QD} = I_{UV} \times QAE \times QCE \ . \tag{5}$$

As pointed out in Fig. 5(c), a higher QAE obtained by increasing the QD concentration would simultaneously reduce the QCE, demonstrating a more serious reabsorption loss. As for this LED II structure, the BN coating is mainly beneficial to the reduction of the UV light (I_{UV}) loss from the LED chip and the improvement of QAE, which is conducive to the I_{QD} improvement owing to the secondary excitation of QD resulted from recycling UV light. Meanwhile, this enhanced secondary excitation of QDs would further reduce the QCE due to the increase in reabsorption loss just similar to the strategy of increased QD concentration, which is proved by the calculated QCE in Fig. 8(b). The QCE of LED with 15% BN concentration is reduced by 20.2% compared with conventional LED. As the secondary excitation is hard to precisely control in order to balance the QAE and QCE, instead, we solve this issue by simply optimizing the QD concentration in the case with secondary excitation.

Authorized licensed use limited to: SOUTH CHINA UNIVERSITY OF TECHNOLOGY. Downloaded on April 06,2021 at 08:55:24 UTC from IEEE Xplore. Restrictions apply.

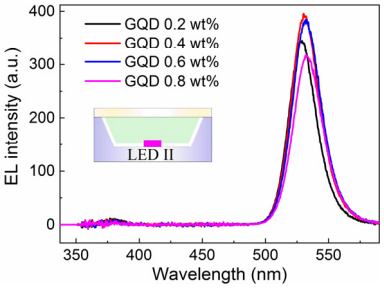

Fig. 9. EL spectra of LED II with different GQD concentration.

The QD concentration is optimized in LED II structure, as shown in Fig. 9. The QD emission intensity shows the best improvement at 0.4 wt% QD concentration, then it decreases with a higher QD concentration. The optimal QD concentration in LED II (0.4 wt%) is further reduced compared with the conventional LED I devices (0.6 wt%) to achieve the maximum QD emission intensity. As pointed out in Fig. 5(c), a lower QD concentration is more beneficial to improve the QCE; the QCE of 0.4 wt% QD concentration is ∼10% higher than of the 0.6 wt% QD concentration. Therefore, the LED II structure can attain the maximum QD emission intensity with a higher QCE, which is beneficial to reduce the reabsorption loss of QDs.

In order to clearly show the role of BN coating and UV-R filter in LED II structure, the radiant flux of the QD-LED only with a UV-R filter, the QD-LED only with a BN coating, and the QD-LED with a combination strategy of UV-R filter and BN coating are compared with that of the original QD-LED, respectively, as shown in Fig. 10(b)–(d). All of these devices adopt the optimal QD concentration of 0.4 wt% in LED II for the package. In Fig. 10(b), the QD-LED only with a UV-R filter largely decreases the radiant flux of UV light by 98.3% while only increases that of the green light by 3.8% compared with the original LED, which is attributed to the reflective filtering effect of the UV-R filter. As for BN coating shown in Fig. 10(c), the QD-LED only with a BN coating slightly reduces the radiant flux of UV light by 12.3% while largely increases that of green light by 33.4%, which is attributed to the secondary excitation of QDs by the recycling UV light. As for the combination sample shown in Fig. 10(d), LED II shows the best performance that the radiant flux of UV light reduces by 98.2% while the radiant flux of green light increases by 34.8%, respectively. Therefore, the positive effect of BN coating and UV-R filter could be maintained after the combination in QD-LEDs, achieving the lowest UV light intensity and the highest QD emission intensity as shown in Fig. 10(a).

C. Strategy Comparisons for Eliminating Residual UV Excitation Light

As discussed above, both LED structures could eliminate the residual UV excitation light by different strategies. The LED I structure can eliminate residual UV excitation light by increasing the QD concentration, while the LED II structure using a UV-R filter. As shown in Fig. 11(a), the EL spectra of these two different strategies are compared. All these LED structures easily eliminate the residual UV excitation light

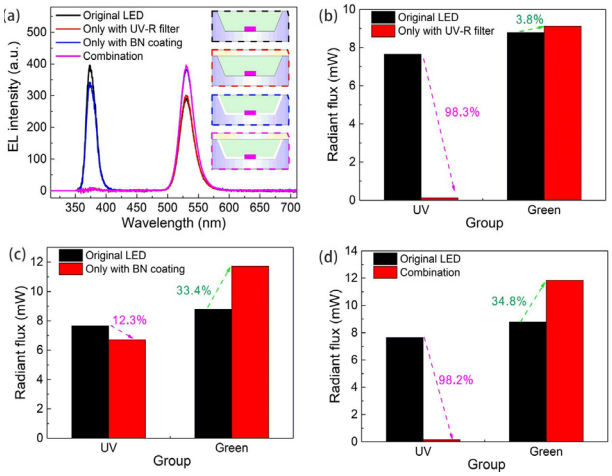

Fig. 10. (a) EL spectra of LED with fixed QD concentration (0.4 wt%) under different package conditions. Comparison of UV and green emission intensity: (b) original LED and LED only with a UV-R filter, (c) original LED and LED only with BN coating, and (d) original LED and LED with the combination (BN coating and a UV-R filter).

close to zero. However, the QD emission peak has a significant redshift in LED I structure owing to the serious reabsorption effect. Sorting from low to high, the QD emission intensity of these two LEDs is: LED I < LED II. Their QPCE and QP are also concluded in Fig. 11(b). Their detailed comparisons are concluded in Table I. All these samples achieve an excellent high QP up to 98.8%, while the green emission intensity of LED II is 82.0% higher than that of the LED I structure. Although the elimination of UV peaks could be achieved by a high concentration QDs, the QPCE is significantly reduced. In contrast, LED II could attain high QP and QPCE at the same time. These results are attributed to the better management of the recycling UV light and reabsorption loss considering the secondary excitation of QDs. Therefore, the combination strategy (LED II) is the best way to eliminate the residual UV excitation light while enhancing QD emission intensity.

This strategy also works equally well for red QD-LED devices, which is compared with the conventional LED I, as concluded in Table I. For RQDs, due to their strong ability to absorb UV light, the concentration of 1.5 wt% can basically eliminate the residual UV excitation peak, which is much lower than GQDs. Under similar QP, the QPCE of red LED II is enhanced to 1.38 times compared with that of LED I. Meanwhile, the red emission intensity of LED II is 36.8% higher than that of LED I. When comparing LED I with LED II, the QD concentration of GQD-LED has changed significantly while that of RQD-LED is relatively less obvious. The QCE of QDs is closely related to QD concentration. Therefore, compared to the RQDs, the QCE of the GQDs changes more obviously from LED I to LED II, resulting in a higher QD emission improvement. Although the improvement of RQD-LED is less obvious than that of GQD-LED, this combined strategy basically eliminates residual UV excitation peaks and effectively improving the emission intensity of RQDs, which is also quite valuable for display applications. In addition, the concentration and amount of QDs used in LED II are the lowest, which is conducive to reduce the cost of QD-LED devices.

Authorized licensed use limited to: SOUTH CHINA UNIVERSITY OF TECHNOLOGY. Downloaded on April 06,2021 at 08:55:24 UTC from IEEE Xplore. Restrictions apply.

TABLE I
COMPARISON OF LED STRUCTURES ELIMINATING RESIDUAL UV EXCITATION LIGHT

Group	Structure	QD / wt%	Filter	BN coating / wt%	QD amount / mg	QP / %	QPCE / %	QD emission improvement / %
Green LED	LED I	4.8	-	-	11	99.2	10.2	-
	LED II	0.4	UV-R	15	8	98.8	18.6	82.0
Red LED	LED I	1.5	-	-	11	94.0	6.5	-
	LED II	0.7	UV-R	15	8	99.4	9.0	36.8

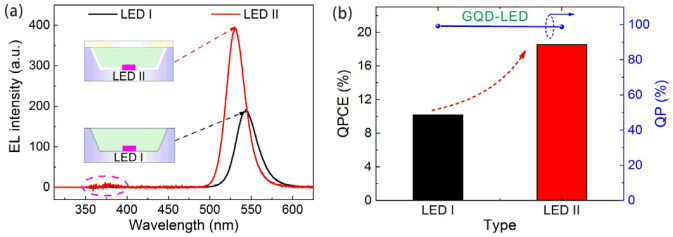

Fig. 11. (a) EL spectra. (b) QPCE and QP of GQD-LED with different LED structures.

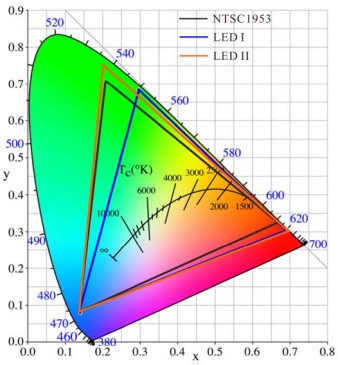

Fig. 12. Comparison of the color gamut of LED I and LED II after eliminating the residual UV excitation peak.

For display applications, the color gamut is one of the key parameters. The color gamut of QD-LED using optimized LED I and LED II structure is provided to further compare the ability to eliminate the intensity of the residual UV excitation peak. Taking NTSC1953 as the baseline, the color coordinate of blue light follows the standard of NTSC1953; the color coordinates of green light and red light are obtained from the QD-LED devices. As shown in Fig. 12, the color coordinates of the green light with different device structure exhibit an obvious difference. This is because, for the device structure of LED I, GQDs tend to aggregate due to the high GQDs concentration (4.8 wt%), which results in a redshift of the emission wavelength. The color gamut of LED I and LED II is 94.6% and 114.2% NTSC1953 standard, respectively. This result suggested that the color gamut of LED II using the proposed combined strategy is 19.6% higher than that of traditional LED I, which is mainly due to the elimination of residual UV excitation peaks, so the features of high color purity of QDs can be fully utilized. Therefore, through the combination strategy, the light output property of QD-LED devices is increased, with the color gamut to be further optimized as well. The above results show practical value for display applications.

Furthermore, the thermal distribution images of the widely used LED I and the proposed LED II under steady state were captured by infrared thermal imager at 100-mA currents.

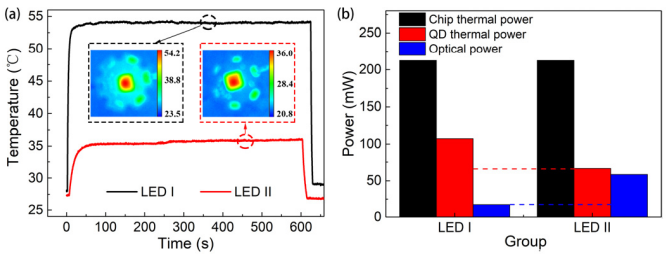

Fig. 13. (a) Infrared temperature of LED I and LED II under 100-mA current, inset image is the infrared image after stabilization. (b) Chip thermal power, QD thermal power and optical power of LED I and LED II under 100 mA.

For LED I, the maximum temperature of the infrared image represents the QD temperature; for LED II, the maximum surface temperature is the temperature of the UV-R filter. Using the simulation method [30], a thermal simulation for an optimized LED II device was conducted. The surface temperature of the UV-R filter (36.6 °C) and the maximum QD temperature (37.7 °C) are relatively close, so the infrared experimental temperature could be used to characterize the approximate temperature of the internal QD. As shown in Fig. 13(a), the maximum temperature of LED I is 54.2 °C, while the maximum temperature of LED II is only 36.0 °C; the latter is much lower than that of LED I. These results indicate that LED II has an advantage of enhancing thermal performance. In LED devices, electrical power is mainly converted into optical power and thermal power. The thermal power of UVLED device without packaging QDs is 212.5 mW at 100 mA current, referred to as chip thermal power. In LED I and LED II samples, the thermal power could be mainly divided into chip thermal power and QD thermal power. As shown in Fig. 13(b), the optical power, chip thermal power, and QD thermal power are analyzed separately [31], [32]. Specifically, the QD thermal power of LED I and LED II is 107.5 and 66.3 mW, respectively. The lower QD thermal power of LED II is attributed to the higher QCE of QDs with a lower QD concentration, supported by the increased optical power. This reveals the heat power generation from QDs is lower in the LED II structure, which is consistent with the results of infrared temperature shown in Fig. 13(a).

IV. CONCLUSION

To eliminate the residual UV excitation light in UV-excited QD-LED devices, two typical types of LED structures are investigated in detail. LED I denotes an LED device that contains only a QDs package; LED II denotes a combined structure of a BN reflective coating and a UV-R filter for a QDs package. LED I could obtain a high QP of 99.2%, however, it significantly reduces the QCE using a high QD concentration package. The LED II is proposed by combining

Authorized licensed use limited to: SOUTH CHINA UNIVERSITY OF TECHNOLOGY. Downloaded on April 06,2021 at 08:55:24 UTC from IEEE Xplore. Restrictions apply.

the BN coating with a UV-R filter. The UV-R filter is used to eliminate the residual UV excitation light while passing through QD emission; the BN reflective coating is essential to reduce the initial UV intensity loss and increase QAE, which in turn generates much more QD emission. Moreover, a higher BN concentration is beneficial to increase the recycling UV light combined with the UV-R filter, thereby further increasing the secondary excitation of QDs and leading to more serious reabsorption loss. After careful optimization of the QD concentration in LED II structure, the negative reabsorption effect is reduced, and a higher QD emission intensity is achieved. Under a similar QP of ∼99.0% (almost no residual UV excitation light), the green emission intensity from QDs of LED II is 82.0% higher than the LED I structure, which works equally well for red QD-LED devices. Under similar QP, the red emission intensity of LED II is 36.8% higher than that of LED I. Besides, the color gamut of the proposed LED II is as high as 114.2%, which is 19.6% higher than traditional LED I. The heat power generation from QDs is also lower in the LED II structure. This study provides a better understanding of residual UV excitation light elimination and QD emission intensity enhancement in QD-LED devices, as well as a reliable strategy for solving this problem, which is conducive to promoting the development of QDs in the field of display devices.

REFERENCES

[1] E. F. Schubert and J. K. Kim, "Solid-state light sources getting smart," *Science*, vol. 308, no. 5726, p. 1274, May 2005, doi: 10.1126/science.1108712.

[2] S. Pimputkar, J. S. Speck, S. P. Denbaars, and S. Nakamura, "Prospects for LED lighting," *Nature Photon.*, vol. 3, no. 4, pp. 180–182, Apr. 2009, doi: 10.1038/nphoton.2009.32.

[3] E. Jang, S. Jun, H. Jang, J. Lim, B. Kim, and Y. Kim, "White-light-emitting diodes with quantum dot color converters for display backlights," *Adv. Mater.*, vol. 22, no. 28, pp. 3076–3080, Jul. 2010, doi: 10.1002/adma.201000525.

[4] W. Huang *et al.*, "Local dimming algorithm and color gamut calibration for RGB LED backlight LCD display," *Opt. Laser Technol.*, vol. 43, no. 1, pp. 214–217, Feb. 2011, doi: 10.1016/j.optlastec.2010.06.016.

[5] C. Peng, X. Li, Z. Pu, L. Xiong, and X. Liu, "RGB high brightness LED modules for projection display application," *J. Display Technol.*, vol. 7, no. 8, pp. 448–453, Aug. 2011, doi: 10.1109/JDT.2011.2132693.

[6] Z. Li *et al.*, "Study on the thermal and optical performance of quantum dot white light-emitting diodes using metal-based inverted packaging structure," *IEEE Trans. Electron Devices*, vol. 66, no. 7, pp. 3020–3027, Jul. 2019, doi: 10.1109/TED.2019.2917010.

[7] L. Wang *et al.*, "Highly efficient narrow-band green and red phosphors enabling wider color-gamut LED backlight for more brilliant displays," *Opt. Exp.*, vol. 23, no. 22, pp. 28707–28717, Nov. 2015, doi: 10.1364/OE.23.028707.

[8] S. Jun, J. Lee, and E. Jang, "Highly luminescent and photostable quantum dot–silica monolith and its application to light-emitting diodes," *ACS Nano*, vol. 7, no. 2, pp. 1472–1477, Jan. 2013, doi: 10.1021/nn3052428.

[9] Z. Li *et al.*, "Investigation of light-extraction mechanisms of multi-scale patterned arrays with rough morphology for GaN-based thin-film LEDs," *IEEE Access*, vol. 7, pp. 73890–73898, Jun. 2019, doi: 10.1109/ACCESS.2019.2921058.

[10] Z. Luo, Y. Chen, and S.-T. Wu, "Wide color gamut LCD with a quantum dot backlight," *Opt. Exp.*, vol. 21, no. 22, pp. 26269–26284, Oct. 2013, doi: 10.1364/OE.21.026269.

[11] R. Zhu, Z. Luo, H. Chen, Y. Dong, and S. T. Wu, "Realizing Rec. 2020 color gamut with quantum dot displays," *Opt. Exp.*, vol. 23, no. 18, pp. 23680–23693, Sep. 2015, doi: 10.1364/OE.23.023680.

[12] H.-W. Chen *et al.*, "Going beyond the limit of an LCD's color gamut," *Light: Sci. Appl.*, vol. 6, no. 9, Sep. 2017, Art. no. e17043, doi: 10.1038/lsa.2017.43.

[13] K. H. Loo, Y. M. Lai, S. C. Tan, and K. T. Chi, "On the color stability of phosphor-converted white LEDs under DC, PWM, and bilevel drive," *IEEE Trans. Power Electron.*, vol. 27, no. 2, pp. 974–984, Feb. 2012, doi: 10.1109/TPEL.2010.2086080.

[14] Z. Li *et al.*, "Highly efficient and water-stable lead halide perovskite quantum dots using superhydrophobic aerogel inorganic matrix for white light-emitting diodes," *Adv. Mater. Technol.*, vol. 5, no. 2, Feb. 2020, Art. no. 1900941, doi: 10.1002/admt.201900941.

[15] X. Lei, H. Zheng, X. Guo, J. Chu, S. Liu, and P. Liu, "Optical performance enhancement of quantum dot-based light-emitting diodes through an optimized remote structure," *IEEE Trans. Electron Devices*, vol. 63, no. 2, pp. 691–697, Feb. 2016, doi: 10.1109/TED.2015.2508026.

[16] J. Li, Y. Tang, Z. Li, X. Ding, and L. Lin, "Largely enhancing luminous efficacy, color-conversion efficiency, and stability for quantum-dot white LEDs using the two-dimensional hexagonal pore structure of SBA-15 mesoporous particles," *ACS Appl. Mater. Interfaces*, vol. 11, no. 20, pp. 18808–18816, Apr. 2019, doi: 10.1021/acsami.8b22298.

[17] C. Yan, X. Du, J. Li, X. Ding, Z. Li, and Y. Tang, "Effect of excitation wavelength on optical performances of quantum-dot-converted light-emitting diode," *Nanomaterials*, vol. 9, no. 8, p. 1100, Aug. 2019, doi: 10.3390/nano9081100.

[18] K. Zhang, D. Peng, K. M. Lau, and Z. Liu, "Fully-integrated active matrix programmable UV and blue micro-LED display system-on-panel (SoP)," *J. Soc. Inf. Display*, vol. 25, no. 4, pp. 240–248, Apr. 2017, doi: 10.1002/jsid.550.

[19] T. J. McMillan, E. Leatherman, A. Ridley, J. Shorrocks, and J. R. Whiteside, "Cellular effects of long wavelength UV light (UVA) in mammalian cells," *J. Pharmacy Pharmacol.*, vol. 60, no. 8, pp. 969–976, Aug. 2008, doi: 10.1211/jpp.60.8.0004.

[20] D. C. Holzman, "What's in a color? The unique human health effects of blue light," *Environ. Health Perspect.*, vol. 118, no. 1, pp. A22–A27, Jan. 2010, doi: 10.1289/ehp.118-a22.

[21] F. Falchi *et al.*, "The new world atlas of artificial night sky brightness," *Sci. Adv.*, vol. 2, no. 6, Jun. 2016, Art. no. e1600377, doi: 10.1126/sciadv.1600377.

[22] G.-S. Chen, B.-Y. Wei, C.-T. Lee, and H.-Y. Lee, "Monolithic red/green/blue micro-LEDs with HBR and DBR structures," *IEEE Photon. Technol. Lett.*, vol. 30, no. 3, pp. 262–265, Feb. 1, 2018, doi: 10.1109/LPT.2017.2786737.

[23] H.-Y. Lin *et al.*, "Optical cross-talk reduction in a quantum-dot-based full-color micro-light-emitting-diode display by a lithographic-fabricated photoresist mold," *Photon. Res.*, vol. 5, no. 5, pp. 411–416, Oct. 2017, doi: 10.1364/prj.5.000411.

[24] J.-S. Li, Y. Tang, Z.-T. Li, K. Cao, C.-M. Yan, and X.-R. Ding, "Full spectral optical modeling of quantum-dot-converted elements for light-emitting diodes considering reabsorption and reemission effect," *Nanotechnology*, vol. 29, no. 29, May 2018, Art. no. 295707, doi: 10.1088/1361-6528/aac1b0.

[25] H. Chen *et al.*, "A novel randomly textured phosphor structure for highly efficient white light-emitting diodes," *Nanosc. Res. Lett.*, vol. 7, no. 1, p. 188, 2012, doi: 10.1186/1556-276x-7-188.

[26] J.-S. Li, Y. Tang, Z.-T. Li, W.-Q. Kang, X.-R. Ding, and B.-H. Yu, "Study on reabsorption properties of quantum dot color convertors for light-emitting diode packaging," *J. Electron. Packag.*, vol. 141, no. 4, Dec. 2019, doi: 10.1115/1.4044475.

[27] J. R. Oh, S. H. Cho, Y. H. Lee, and Y. R. Do, "Enhanced forward efficiency of $Y_3Al_5O_{12}$:Ce^3+ phosphor from white light-emitting diodes using blue-pass yellow-reflection filter," *Opt. Exp.*, vol. 17, no. 9, pp. 7450–7457, Apr. 2009, doi: 10.1364/OE.17.007450.

[28] C. Yan, Q. Zhao, J. Li, X. Ding, Y. Tang, and Z. Li, "Improving optical performance of ultraviolet light-emitting diodes by incorporating boron nitride nanoparticles," *Electronics*, vol. 8, no. 8, p. 835, Jul. 2019, doi: 10.3390/electronics8080835.

[29] L. Zhang *et al.*, "Development of an Al_2O_3 filled composite for the bracket of ultraviolet light-emitting diodes (UV-LEDs)," *Opt. Mater.*, vol. 83, pp. 356–362, Sep. 2018, doi: 10.1016/j.optmat.2018.06.033.

[30] B. Xie *et al.*, "Targeting cooling for quantum dots in white QDs-LEDs by hexagonal boron nitride platelets with electrostatic bonding," *Adv. Funct. Mater.*, vol. 28, no. 30, Jun. 2018, Art. no. 1801407, doi: 10.1002/adfm.201801407.

[31] B. Xie, R. Hu, X. Yu, B. Shang, Y. Ma, and X. Luo, "Effect of packaging method on performance of light-emitting diodes with quantum dot phosphor," *IEEE Photon. Technol. Lett.*, vol. 28, no. 10, pp. 1115–1118, May 15, 2016, doi: 10.1109/LPT.2016.2531794.

[32] Z.-T. Li, J.-X. Li, J.-S. Li, X.-W. Du, C.-J. Song, and Y. Tang, "Thermal impact of LED chips on quantum dots in remote-chip and on-chip packaging structures," *IEEE Trans. Electron Devices*, vol. 66, no. 11, pp. 4817–4822, Nov. 2019, doi: 10.1109/TED.2019.2941911.

Authorized licensed use limited to: SOUTH CHINA UNIVERSITY OF TECHNOLOGY. Downloaded on April 06,2021 at 08:55:24 UTC from IEEE Xplore. Restrictions apply.